arXiv:hep-lat/9903038v1 29 Mar 1999

Dual Higgs Mechanism based on the Dual Gauge Formalism in the Lattice QCD

Atsunori Tanaka and Hideo Suganuma

Research Center for Nuclear Physics (RCNP), Osaka University

Mihogaoka 10-1, Ibaraki, Osaka 567-0047, Japan

E-mail: suganuma@rcnp.osaka-u.ac.jp

Abstract

We study the dual Higgs mechanism induced by monopole condensation based on the dual gauge formalism in the maximally abelian (MA) gauge in the lattice QCD. To examine "monopole condensation" in QCD, we study the monopole part or the monopole-current system appearing in the MA gauge by extracting the dual gluon field B_μ. First, we investigate the inter-monopole potential using the dual Wilson loop in the lattice QCD simulation. In the monopole part in the MA gauge, the inter-monopole potential is found to be flat, and can be fitted as the Yukawa potential in the infrared region. From more detailed analysis of the inter-monopole potential considering the monopole size, we estimate the effective dual-gluon mass $m_B \simeq 0.5$GeV and the effective monopole size $R_{\rm M} \simeq 0.2$fm. Second, we study the dual gluon propagator $G^D_{\mu\nu}(x-y) \equiv \langle B_\mu(x)B_\nu(y)\rangle_{\rm MA}$ in the MA gauge, and find that $G^D_{\mu\mu}$ behaves as the massive vector-boson propagator with $m_B \simeq 0.4$ GeV in the infrared region. The effective-mass acquirement of the dual gluon field B_μ at the long distance can be regarded as the lattice QCD evidence of "infrared monopole condensation" in the MA gauge.

PACS number(s):12.38.Gc, 12.38.Aw, 11.15.Ha

Typeset using REVTEX

I. INTRODUCTION

Quantum chromo-dynamics (QCD) is the fundamental theory of the strong interaction and exhibits the interesting phenomena such as color confinement and dynamical chiral-symmetry breaking (DχSB) [1–7]. The QCD Lagrangian has the SU(N_c) local symmetry and is described by the quark field q and the gluon field A_μ as

$$\mathcal{L}_{QCD} = -\frac{1}{2}\mathrm{tr}(G_{\mu\nu}G^{\mu\nu}) + \bar{q}(i\not{D} - m_q)q, \tag{1}$$

where $G_{\mu\nu}$ denotes the SU(N_c) field strength $G_{\mu\nu} \equiv \frac{1}{ie}[D_\mu, D_\nu]$ with the covariant-derivative operator $D_\mu \equiv \partial_\mu + ieA_\mu$ [1]. In QCD, the asymptotic freedom is one of the most important features in QCD [1–3], and the QCD gauge-coupling constant e becomes small in the ultraviolet region. On the other hand, in the low-energy region, the gauge-coupling constant e becomes large, and there arise the nonperturbative-QCD (NP-QCD) phenomena like color confinement and DχSB corresponding to the strong-coupling nature. These NP-QCD phenomena are extremely difficult to understand in the analytical manner from QCD and have been studied by using the effective models [6] or the lattice QCD simulation [7].

In the lattice formalism, space-time coordinates are discretized with the lattice spacing a, and the theory is described by the link variable $U_\mu(s) \equiv e^{iaeA_\mu(s)} \in \mathrm{SU}(N_c)$. For instance, the standard lattice action is given as

$$S = \beta \sum_{s,\mu>\nu} [1 - \frac{1}{2N_c}\mathrm{tr}\{U_{\mu\nu}(s) + U^\dagger_{\mu\nu}(s)\}], \ \beta \equiv \frac{2N_c}{e^2} \tag{2}$$

where $U_{\mu\nu}(s)$ is the plaquette variable defined as $U_{\mu\nu}(s) \equiv U_\mu(s)U_\nu(s+\mu)U^\dagger_\mu(s+\nu)U^\dagger_\nu(s)$. The lattice QCD Monte Carlo simulation is based on the numerical calculation of the QCD partition functional, and it is one of the most reliable methods directly from QCD. In the lattice QCD, nonperturbative quantities like the quark confinement potential, the chiral condensate $\langle\bar{q}q\rangle$ and low-lying hadron masses are well reproduced [7]. However, one cannot understand the confinement mechanism only by looking on the result obtained by the lattice QCD.

Recently, the lattice QCD simulation has shed light on the confinement mechanism in terms of the dual-superconductor picture, which was first proposed by Nambu,'t Hooft and Mandelstam in the middle of 1970's [8–10]. In this scenario, quark confinement can be understood with the dual version of the superconductivity. In the ordinary superconductor, the Meissner effect occurs by condensation of the Cooper-pair with the electric charge [11]. Consider existence of the magnetic charges with the opposite sign immersed in the superconductor, then the magnetic flux is squeezed like a tube between the magnetic charges, and the magnetic potential between them becomes linear as the result of the Meissner effect [11]. On the other hand, the confinement force between the color-electric charge is characterized by the universal physical quantity of the string tension $\sigma = 0.89 \sim 1$ GeV/fm, which is evaluated from the Regge trajectory of hadrons and the lattice QCD simulations. This string tension is brought by one-dimensional squeezing of the color-electric flux in the QCD vacuum [25]. In the dual-superconductor scenario [8], the QCD vacuum is assumed as the dual version of the superconductor, and the dual Meissner effect brings the one-dimensional flux tube [12] between the quark and the anti-quark, which leads to the linear confinement potential [4–8,13].

The dual Higgs mechanism, however, requires "color-magnetic monopole condensation" as the dual version of electric condensation in the superconductor, although QCD dose not include the color-magnetic monopole as the elementary degrees of freedom. On the appearance of magnetic monopoles from QCD, 't Hooft showed that QCD is reduced to an abelian gauge theory with magnetic monopoles by taking the abelian gauge, which fixes the partial gauge symmetry $\mathrm{SU}(N_C)/\mathrm{U}(1)^{N_c-1}$ through the diagonalization of a gauge-dependent variable [14]. Here, the color-magnetic monopole appears as the topological object corresponding to the nontrivial homotopy group $\pi_2(\mathrm{SU}(N_c)/\mathrm{U}(1)^{N_c-1})$=$Z_\infty^{N_c-1}$.

Recent lattice QCD studies show abelian dominance [15], which means that NP-QCD phenomena like confinement [18,19] and DχBS [20,21] are almost described only by the diagonal gluon component in the maximally abelian (MA) gauge [16,17]. The MA gauge is a sort of the abelian gauge where off-diagonal gluon components are minimized by the gauge transformation. In the MA gauge, physical information of the gauge configuration is maximally concentrated into the diagonal gluon component. As for the NP-QCD phenomena, QCD can be well approximated by the abelian projected QCD (AP-QCD), which is the abelian gauge theory extracted from QCD in the MA gauge by removing the off-diagonal gluon [16,17].

AP-QCD includes not only electric currents j_μ but also magnetic currents k_μ, and can be decomposed into the photon part and the monopole part corresponding to the separation of j_μ and k_μ, respectively [22,23]. In other words, AP-QCD consists of the two parts. The photon part of AP-QCD (photon-projected QCD) is the abelian gauge theory only with electric currents j_μ like the ordinary QED. On the other hand, the monopole part of AP-QCD (monopole-projected QCD) only includes monopole currents k_μ. The lattice QCD studies show monopole dominance, which means that NP-QCD phenomena are almost described only by the monopole projected QCD [20,23–27]. In particular, the lattice QCD simulation numerically shows that the monopole current k_μ is responsible for the electric confinement and j_μ does not contribute to it in the MA gauge [23–25]. Since we are interested in the infrared physics such as confinement and its mechanism in the QCD vacuum, we discard the off-diagonal gluon and the photon part in the MA gauge as the irrelevant ingredients, because they do not contribute to the quark confinement. Then, we concentrate ourselves on the monopole part in the MA gauge for the study of the confinement mechanism.

Then, the remaining problem is whether "monopole condensation" occurs in the QCD vacuum or not. In this paper, we perform the SU(2) lattice QCD simulation in the MA gauge, and extract the monopole current k_μ as the relevant degrees of freedom for confinement. Then, we numerically derive the dual gluon field B_μ from k_μ [28,29], and investigate the effective-mass acquirement of the dual gluon B_μ in the QCD vacuum by examining the inter-monopole potential and the dual gluon propagator.

II. ABELIAN PROJECTION AND MONOPOLE PROJECTION IN THE LATTICE QCD FORMALISM

A. Abelian-Projected QCD in the MA gauge

Recent studies with the lattice QCD Monte Carlo simulation have revealed the abelian dominance and the monopole dominance in the maximally abelian (MA) gauge for the non-perturbative QCD (NP-QCD) phenomena such as confinement, dynamical chiral-symmetry breaking and instantons [18–27]. In the SU(2) lattice formalism, the MA gauge fixing is achieved by maximizing

$$R = \frac{1}{2}\mathrm{tr}\sum_{s,\mu}[\tau^3 U_\mu(s)\tau^3 U_\mu^\dagger(s)] = \sum_{s,\mu}\left[1-2\left(\{U_\mu^1(s)\}^2+\{U_\mu^2(s)\}^2\right)\right] \tag{3}$$

by the SU(2) gauge transformation,

$$U_\mu \to U_\mu^{\mathrm{MA}} = V(s)U_\mu(s)V^\dagger(s+\mu), \tag{4}$$

where $V(s)$ and $V(s+\mu)$ are the gauge functions located at the starting and end points of the link variable $U_\mu(s)$. In this gauge, the absolute value of off-diagonal components $U_\mu^1(s)$ and $U_\mu^1(s)$ are forced to be small as possible using the gauge degrees of freedom.

In accordance with the Cartan decomposition, the SU(2) link variable $U_\mu(s)$ is factorized as

$$U_\mu^{\mathrm{MA}}(s) = M_\mu(s)u_\mu(s)\ , \tag{5}$$

$$M_\mu \equiv \exp[i(\theta_\mu^1\tau^1+\theta_\mu^2\tau^2)], \quad u_\mu(s) \equiv \exp[i(\theta_\mu^3\tau^3)], \tag{6}$$

where $u_\mu \in \mathrm{U}(1)_3$ and $M_\mu \in \mathrm{SU}(2)/\mathrm{U}(1)_3$ correspond to the diagonal part and the off-diagonal part of the gluon field, respectively. In the continuum limit, the angle variable θ_μ^a goes to the gluon field A_μ^a as $\theta_\mu^a \to \frac{1}{2}eaA_\mu^a$. The off-diagonal factor $M_\mu(s)$ is rewritten as

$$M_\mu(s) = e^{i(\theta_\mu^1\tau^1+\theta_\mu^2\tau^2)} = \begin{pmatrix} \cos\theta_\mu & -\sin\theta_\mu e^{-i\chi_\mu} \\ \sin\theta_\mu e^{i\chi_\mu} & \cos\theta_\mu \end{pmatrix}. \tag{7}$$

with

$$\theta_\mu \equiv \mathrm{mod}_{\pi/2}\sqrt{(\theta^1_\mu)^2+(\theta^2_\mu)^2}, \qquad \chi_\mu \equiv \tan^{-1}\frac{\theta^1_\mu}{\theta^2_\mu}. \tag{8}$$

Here, the parameter ranges are usually taken as

$$\theta_\mu \in [0,\frac{\pi}{2}],\ \chi_\mu \in [0,2\pi),\ \theta^3_\mu \in [0,2\pi), \tag{9}$$

which provides the one-to-one correspondence to the SU(2) group element. Under the abelian gauge transformation with $v(s) \in \mathrm{U}(1)_3$, $M_\mu(s)$ and $u_\mu(s)$ are transformed as

$$M_\mu(s) \to M^v_\mu(s) = v(s)M_\mu(s)v^\dagger(s), \tag{10}$$

$$u_\mu(s) \to u^v_\mu(s) = v(s)u_\mu(s)v^\dagger(s+\mu), \tag{11}$$

to keep the form of Eq.(6) for $M^v_\mu \in \mathrm{SU}(2)/\mathrm{U}(1)_3$ and $u^v_\mu \in \mathrm{U}(1)_3$. Then, $M_\mu(s)$ behaves as the charged matter field and the abelian link-variable

$$u_\mu(s) = \begin{pmatrix} e^{i\theta^3_\mu} & 0 \\ 0 & e^{-i\theta^3_\mu} \end{pmatrix} \tag{12}$$

behaves as a abelian gauge field with respect to the residual abelian gauge symmetry.

As a remarkable feature of the MA gauge, the abelian dominance holds for the NP-QCD phenomena such as quark confinement and chiral-symmetry breaking [18–21]. Here, we call abelian dominance for an operator $\hat{O}$, when the expectation value $\langle O[U_\mu]\rangle$ is almost equal to the expectation value $\langle O[u_\mu]\rangle_{\mathrm{MA}}$, where off-diagonal gluons are dropped off in the MA gauge. For instance, the abelian string tension $\sigma_{\mathrm{Abel}} \equiv \langle \sigma(U_\mu)\rangle_{\mathrm{MA}}$ in the MA gauge is almost equal to $\sigma_{\mathrm{SU(2)}} \equiv \langle\sigma(U_\mu)\rangle$ as $\sigma_{\mathrm{Abel}} \simeq 0.92\sigma_{\mathrm{SU(2)}}$ for $\beta \simeq 2.5$ in the lattice QCD [24,25]. Thus, NP-QCD phenomena are almost reproduced only by the abelian link variable u_μ, and off-diagonal gluon components θ^1_μ, θ^2_μ do not contribute to NP-QCD in the MA gauge. Hence, as long as the infrared physics is concerned, QCD in the MA gauge can be approximated by the abelian projected QCD (AP-QCD), where the SU(2) gluon field $\theta^a_\mu\tau^a$ is replaced by the abelian gluon field $\theta^3_\mu\tau^3$. In other words, AP-QCD is the abelian gauge theory keeping essence of NP-QCD, and is extracted from QCD in the MA gauge. Hereafter, we pay attention to the AP-QCD described by θ^3_μ in the MA gauge.

B. Decomposition of AP-QCD into Monopole Part and Photon Part

The abelian-projected QCD (AP-QCD) includes not only the color-electric current j_μ but also the color-magnetic monopole current k_μ [14]. In the Maxwell equations with j_μ and k_μ, the field strength $\theta_{\mu\nu}^{\rm Abel}$ satisfies as

$$\partial_\mu \theta_{\mu\nu}^{\rm Abel} = j_\nu \tag{13}$$

$$\partial_\mu \, {}^*\theta_{\mu\nu}^{\rm Abel} = k_\nu \tag{14}$$

with ${}^*\theta_{\mu\nu}^{\rm Abel} \equiv \frac{1}{2}\varepsilon_{\mu\nu\rho\sigma}\theta_{\rho\sigma}^{\rm Abel}$. In the presence of both j_μ and k_μ, the field strength $\theta_{\mu\nu}^{\rm Abel}$ cannot be described by the simple two-form $\partial_\mu\theta_\nu^3 - \partial_\nu\theta_\mu^3$ with the regular one-form θ_μ^3 [30]. Using the diagonal gluon component θ_μ^3, the abelian field strength $\theta_{\mu\nu}^{\rm Abel}$ is defined by

$$\theta_{\mu\nu}^{\rm Abel} = {\rm mod}_{2\pi}(\partial_\mu\theta_\nu^3 - \partial_\nu\theta_\mu^3) \quad \in [-\pi, \pi), \tag{15}$$

which is U(1)$_3$-gauge invariant. In the continuum limit $a \to 0$, $\theta_{\mu\nu}^{\rm Abel}$ goes to the abelian field strength $F_{\mu\nu}$ in the physical unit as $\theta_{\mu\nu}^{\rm Abel} \to \frac{1}{2}ea^2F_{\mu\nu}$, and therefore the range of $\theta_{\mu\nu}^{\rm Abel}$ is required to include 0. Then, the two-form $\partial_\mu\theta_\nu^3 - \partial_\nu\theta_\mu^3$ can be decomposed as

$$\partial_\mu\theta_\nu^3 - \partial_\nu\theta_\mu^3 = \theta_{\mu\nu}^{\rm Abel} + 2\pi n_{\mu\nu}, \tag{16}$$

where the former part denotes the field strength and the latter part $2\pi n_{\mu\nu}(s) \in 2\pi\mathbf{Z}$ corresponds to the Dirac string on the lattice [22]. Thus, in the ordinary description [30], the system includes the singularity as the Dirac string $2\pi n_{\mu\nu}$, which makes the analysis complicated.

To clarify the roles of j_μ and k_μ to the nonperturbative quantities of QCD, we consider the decomposition of AP-QCD into the photon part and the monopole part, corresponding to the separation of j_μ and k_μ. We call this separation into the photon and monopole parts as the "photon projection" and the "monopole projection", respectively [26,31].

In the lattice formalism, the photon part $\theta_\mu^{\rm Ph}(s)$ and the monopole part $\theta_\mu^{\rm Mo}(s)$ are obtained from $\theta_{\mu\nu}^{\rm Abel}(s)$ and $2\pi n_{\mu\nu}(s)$, respectively,

$$\theta_\mu^{\rm Ph}(s) = \{\Box^{-1}\partial_\nu \theta_{\mu\nu}^{\rm Abel}\}(s) \tag{17}$$

$$\theta_\mu^{\rm Mo}(s) = 2\pi\{\Box^{-1}\partial_\nu n_{\mu\nu}\}(s), \tag{18}$$

using the inverse d'Alembertian $\Box^{-1}$ on the lattice [20,32]. Here, $\Box^{-1}$ is the non-local operator [22,32],

$$\langle s|\Box^{-1}|s'\rangle = -\frac{1}{4\pi^2}\frac{1}{(s-s')^2} \tag{19}$$

which satisfies

$$\Box_s\langle s|\Box^{-1}|s'\rangle = \delta^4(s-s') = \langle s|s'\rangle. \tag{20}$$

The diagonal gluon component $\theta_\mu^3(s)$ is found to be decomposed as

$$\theta_\mu^3(s) = \theta_\mu^{\rm Ph}(s) + \theta_\mu^{\rm Mo}(s) \tag{21}$$

in the Landau gauge, $\partial_\mu \theta_\mu^3(s) = 0$. The field strengths, $\theta_{\mu\nu}^{\rm Ph}$ in the photon part and $\theta_{\mu\nu}^{\rm Mo}$ in the monopole part, are given as

$$\theta_{\mu\nu}^{\rm Ph} = {\rm mod}_{2\pi}(\partial_\mu\theta_\nu^{\rm Ph} - \partial_\nu\theta_\mu^{\rm Ph}) \quad \in [-\pi,\pi) \tag{22}$$

$$\theta_{\mu\nu}^{\rm Mo} = {\rm mod}_{2\pi}(\partial_\mu\theta_\nu^{\rm Mo} - \partial_\nu\theta_\mu^{\rm Mo}) \quad \in [-\pi,\pi) \tag{23}$$

on the lattice, respectively.

In the actual lattice QCD simulation, the monopole current k_μ and the electric current j_μ are slightly modified through the monopole and the photon projections, respectively, due to the numerical error on the lattice. However, these differences are negligibly small in the actual lattice QCD simulation. In fact, $k_\mu^{\rm Mo} \simeq k_\mu$ and $j_\mu^{\rm Mo} \simeq 0$ hold in the monopole part, and $j_\mu^{\rm Ph} \simeq j_\mu$ and $k_\mu^{\rm Ph} \simeq 0$ hold in the photon part within 1% error [26]. Here, we have kept the labels as "*Mo*" and "*Ph*" for the electric current and the monopole current, and we have used $(k_\mu^{\rm Mo}, j_\mu^{\rm Mo})$ and $(k_\mu^{\rm Ph}, j_\mu^{\rm Ph})$ for these currents in the monopole part and the photon part, respectively.

As a remarkable fact, lattice QCD simulations show that nonperturbative quantities such as the string tension, the chiral condensate and instantons are almost reproduced only by the monopole part in the MA gauge, which is called as monopole dominance [23–26]. On the other hand, the photon part dose not contribute these nonperturbative quantities in QCD.

Since we are interested in the NP-QCD phenomena, it is convenient and transparent to extract the relevant degrees of freedom for NP-QCD by removing irrelevant degrees of freedom like the off-diagonal gluons (θ_μ^1*,* θ_μ^2*) and the electric current* j_μ*. Therefore, we concentrate ourselves to the monopole part, which keeps the essence of NP-QCD such as confinement, and we examine whether monopole condensation occurs or not. In other words, our aim is to investigate the feature of the monopole-current system appearing in the MA gauge.*

III. DUAL GAUGE FORMALISM

In the MA gauge, the monopole part carries essence of the nonperturbative QCD like the electric confinement [20,23–27]. Since the monopole part only includes the color-magnetic current k_μ, i.e. j_μ=0, the Maxwell equation in the monopole part becomes

$$\partial_\mu \theta^{\rm Mo}_{\mu\nu} = 0 \tag{24}$$

$$\partial_\mu {}^*\theta^{\rm Mo}_{\mu\nu} = k_\nu, \tag{25}$$

where $\theta^{\rm Mo}_{\mu\nu}$ denotes the field strength in the monopole part. This system resembles the dual version of QED with $j_\mu \neq 0$ and $k_\mu = 0$, and hence it is useful to introduce the dual gluon field $B_\mu(s)$ instead of $\theta^{\rm Mo}_\mu(s)$ in the monopole part for the study of the dual Higgs mechanism in QCD [28].

The dual gluon field B_μ is defined so as to satisfy the definition of the abelian gauge field,

$$\partial_\mu B_\nu - \partial_\nu B_\mu =^* \theta^{\rm Mo}_{\mu\nu}, \tag{26}$$

which is the dual version of the ordinary relation, $F_{\mu\nu} \equiv \partial_\mu A_\nu - \partial_\nu A_\mu$ [29]. The interchange between A_μ and B_μ corresponds to the electro-magnetic duality transformation, $\mathbf{H} \leftrightarrow \mathbf{E}$. Therefore, owing to the absence of j_μ, the dual gauge field B_μ can be introduced without the singularity like the Dirac string. In other words, the absence of j_ν is automatically derived as the dual Bianchi identity,

$$j_\nu = \partial_\mu \theta_{\mu\nu} = \partial_\mu {}^*(\partial \wedge B)_{\mu\nu} = 0. \tag{27}$$

Let us consider the derivation of the dual gauge field B_μ from the monopole current k_μ. Taking the dual Landau gauge $\partial_\mu B_\mu = 0$, the relation $\partial_\mu {}^*\theta^{\rm Mo}_{\mu\nu} = \partial^2 B_\nu - \partial_\nu(\partial_\mu B_\mu) = k_\nu$ becomes a simple form $\Box B_\mu = k_\mu$. Therefore, the dual gluon field $B_\mu(x)$ is obtained as

$$B_\nu(x) = \left(\Box^{-1} k_\nu\right)(x) = \int d^4y \langle x|\Box^{-1}|y\rangle k_\nu(y). = -\frac{1}{4\pi^2}\int d^4y \frac{k_\nu(y)}{(x-y)^2} \tag{28}$$

by using the inverse d'Alembertian $\Box^{-1}$ [22,32]. Here, the dual gauge formalism provides the natural description of the monopole part in terms of the monopole current k_μ and the dual gluon B_μ. Moreover, the dual gauge formalism is useful to examine the dual Higgs mechanism in QCD [28,29].

In the dual superconductor picture in QCD, k_μ and B_μ correspond to the Cooper-pair and the photon in the superconductor, respectively. The Cooper-pair and the photon are essential degrees of freedom which bring the superconductivity. In the superconductor, the photon field A_μ gets the effective mass as the result of Cooper-pair condensation, and this leads to the Meissner effect. Accordingly, the potential between the static electric charges becomes the Yukawa potential $V_Y(r) \propto \frac{e^{-mr}}{r}$ in the ideal superconductor obeying the London equation. Similarly, the dual gluon B_μ is expected to be massive in the the monopole-condensed system, and the mass acquirement of B_μ leads to the dual Meissner effect. In other words, the acquirement of dual gluon mass m_B reflects monopole condensation, and brings electric confinement. Hence, we can investigate the dual Higgs mechanism in QCD by evaluating the dual gluon mass m_B, which is evaluated from the inter-monopole potential.

To estimate the inter-monopole potential, we propose the dual Wilson loop W_D [28,29]. The dual Wilson loop W_D is defined by the line-integral of the dual gluon field B_μ along a closed loop C,

$$W_D(C) \equiv Re[\exp{(i \oint_C B_\mu dx_\mu)}], \tag{29}$$

which is the *dual version of the abelian Wilson loop* $W_{\rm Abel}(C) \equiv Re[\exp{(i \oint_C \theta^3_\mu dx_\mu)}]$. Here, the dual Wilson loop $W_D(R \times T)$ describes the interaction between the monopole-pair with the test magnetic charges $\frac{e}{2}$ and $-\frac{e}{2}$. The inter-monopole potential[1] is obtained from the dual Wilson loop as

$$V_M(R) = -\lim_{T\to\infty} \frac{1}{aT} \ln\langle W_D(R\times T)\rangle \tag{30}$$

---

[1] Rigorously, $V_M(r)$ corresponds to the inter-monopole potential in the monopole part (the monopole-current system) in the MA gauge.

in a similar manner to the extraction of the inter-quark potential from the Wilson loop [4–7].

To summarize, starting from the monopole current k_μ in the MA gauge, we have introduced the dual gluon field B_μ and the dual Wilson loop for the investigation of the dual Higgs mechanism in QCD.

IV. INTER-MONOPOLE POTENTIAL AND DUAL GLUON EFFECTIVE MASS

In this section, we show the numerical result of the lattice QCD simulation. For the study of the dual Higgs mechanism in QCD, we calculate the dual Wilson loop $W_D(R,T)$ and investigate the inter-monopole potential $V_M(r)$ in the MA gauge using the SU(2) lattice with 20^4 and $\beta = 2.2 \sim 2.3$. All measurements are performed at every 100 sweeps after a thermalization of 5000 sweeps using the heat-bath algorithm. We prepare 100 samples of gauge configurations. These simulations have been performed using NEC SX-4 at Computation Center of Osaka University.

In the dual Higgs mechanism, it is essential that the dual gluon field B_μ acquires the effective mass. For investigating the effective-mass acquirement of the dual gluon B_μ which is brought by the monopole condensation, let us extract the inter-monopole potential $V_M(r)$ from the dual Wilson loop $\langle W_D(R,T)\rangle_{\rm MA}$ obtained by the lattice QCD. The dual Wilson loop $\langle W_D(R,T)\rangle_{\rm MA}$ seems to obey the perimeter law rather than the area law for large loops as shown in Fig.1. Since the dual Wilson loop $\langle W_D(R,T)\rangle_{\rm MA}$ satisfies the perimeter law as

$$\ln\langle W_D(R\times T)\rangle_{\rm MA} \simeq -2a(R+T)\cdot\alpha \tag{31}$$

for large R and T, the inter-monopole potential becomes constant 2α in the infinite limit of T,

$$V_M(R) \to \lim_{T\to\infty} \frac{2\alpha}{T}R + 2\alpha = 2\alpha. \tag{32}$$

However, in the actual lattice calculation, we have to take a finite length of T, and hence, the linear part $(2\alpha/T)R$ remains as a lattice artifact. Therefore, it is necessary to subtract this lattice artifact $(2\alpha/T)R$ for evaluating of the inter-monopole potential $V_M(r)$ from $W_D(R,T)$ in the lattice QCD simulation. The parameter α can be estimated from the slope of the dual Wilson loop $\ln\langle W_D(R\times T)\rangle_{\rm MA}$ for large R and T for each lattices. Here, we obtain $\alpha \simeq 0.14$GeV from the dual Wilson loop in Fig.1 for $R,T > 3$ in the lattice unit. After the subtraction of the lattice artifact $(2\alpha/T)R$, we consider the shape of the inter-monopole potential $V_M(r)$ in the lattice QCD in the physical unit with $r \equiv aR$. The inter-monopole potential $V_M(r)$ is short-ranged and flat as shown in Fig.2.

Here, we compare the inter-monopole potential $V_M(r)$ with the Yukawa potential

$$V_Y(r) = -\frac{(e/2)^2}{4\pi}\frac{e^{-m_B r}}{r}. \tag{33}$$

Since the Yukawa potential $V_Y(r)$ satisfies the relation $\ln\{rV_Y(r)\} = -m_B r + const$, we show the logarithm plot of $rV_M(r)$ as the function of r in Fig.3. In the long-distance region, $\ln\{rV_M(r)\}$ seems to decrease linearly with r. From the linear slope of $\ln\{rV_M(r)\}$ in the region of $r \gtrsim 0.4$ fm, the effective mass of the dual gluon B_μ is estimated as $m_B \simeq 0.5$ GeV. As shown in Fig.4, the inter-monopole potential can be fitted by the Yukawa potential $V_Y(r)$ in the long distance region using the dual gluon mass $m_B = 0.5$GeV and the gauge coupling $e = 2.5$.

Finally, we consider the possibility of the monopole size effect, because the monopole is expected to be a soliton like object composed of gluons. In fact, from the recent lattice QCD study, QCD monopoles include large off-diagonal gluons component in their internal region even in the MA gauge [29,31,33]. We introduce the effective size $R_{\rm M}$ of the QCD-monopole, and assume the Gaussian-type distribution of the magnetic charge around its center,

$$\rho(\mathbf{x}; R_{\rm M}) = \frac{1}{(\sqrt{\pi}R_{\rm M})^3}\exp\left(\frac{-|\mathbf{x}|^2}{R_{\rm M}^2}\right). \tag{34}$$

Since the monopole part is an abelian system, simple superposition principle on B_μ is applicable like the Maxwell equation. Therefore, the Yukawa-type potential $V_M(r)$ with the effective size $R_{\rm M}$ of the monopole is expected to be

$$V(\mathbf{x}; R_{\rm M}) = -\frac{(e/2)^2}{4\pi}\int d^3x_1 \int d^3x_2 \rho(\mathbf{x_1}; R_{\rm M})\rho(\mathbf{x_2}; R_{\rm M})\frac{\exp(-m_B|\mathbf{x}-\mathbf{x_1}+\mathbf{x_2}|)}{|\mathbf{x}-\mathbf{x_1}+\mathbf{x_2}|}, \tag{35}$$

or equivalently

$$\begin{aligned} V(r; R_{\rm M}) = &-\frac{(e/2)^2}{\pi^2 R_{\rm M}^6}\int_0^\infty dr_1 \int_0^\infty dr_2 e^{-(r_1^2+r_2^2)/R_{\rm M}^2}\int_0^\pi d\theta_1 \int_0^\pi d\theta_2 \sin\theta_1 \sin\theta_2 \\ &\times \frac{\exp\left[-m_B\sqrt{\{\sqrt{(r-r_2\cos\theta_2)^2+(r_2\sin\theta_2)^2}-r_1\cos\theta_1\}^2+(r_1\sin\theta_1)^2}\right]}{\sqrt{\{\sqrt{(r-r_2\cos\theta_2)^2+(r_2\sin\theta_2)^2}-r_1\cos\theta_1\}^2+(r_1\sin\theta_1)^2}} \end{aligned} \tag{36}$$

where $r \equiv |\mathbf{x} - \mathbf{y}|$ is the distance between the two monopole centers. We apply this potential $V(r; R_{\rm M})$ to the inter-monopole potential $V_M(r)$ in Fig.4. The Yukawa-type potential $V(r; R_{\rm M})$ with the effective monopole size $R_{\rm M} = 0.21$fm seems to fit the inter-monopole potential well in the whole region of the distance r.

Thus, we estimate the dual gluon mass $m_B \simeq 0.5$GeV and the effective monopole size $R_{\rm M} \simeq 0.2$fm by evaluating the inter-monopole potential $V_M(r)$ from $W_D(R, T)$ in the monopole part in the MA gauge. We find the effective mass acquirement of the dual gluon, which is essential for the dual Higgs mechanism in the dual superconductor scenario, and suggest that color confinement is caused by the monopole condensation in the QCD vacuum. The monopole size $R_{\rm M}$ would provide the critical scale for the nonperturbative QCD in terms of the dual Higgs theory, because off-diagonal gluons contribute to the physics and AP-QCD should be modified at the shorter scale than $R_{\rm M}$, as well as the structure of the 't Hooft-Polyakov monopole [2].

V. DUAL GLUON PROPAGATOR AND DUAL GLUON EFFECTIVE MASS

In the previous section, we estimate the dual gluon mass m_B using the inter-monopole potential. The more detailed measurement of m_B from the inter-monopole potential seems difficult because it requires the twice logarithmic-part procedure from the dual Wilson loop [28,29]. As alternative method, we investigate the dual gluon mass m_B through the dual gluon propagator in the lattice QCD.

A. Massive Gauge Field and its Propagator

In this subsection, we consider the general argument on the analytical relation between the massive gauge field and its propagator. To this end, we idealize here the dual gluon field B_μ as a massive vector boson.

The lagrangian for the free massive vector field B_μ in the Proca formalism is written as

$$\mathcal{L}_{\rm Proca} = -\frac{1}{4}(\partial_\mu B_\nu - \partial_\nu B_\mu)^2 - \frac{1}{2} m_B^2 B_\mu^2 \tag{37}$$

in the Euclidean metric [4]. The Proca lagrangian Eq.(37) leads to the field equation [3]

$$\partial_\mu(\partial_\mu B_\nu - \partial_\nu B_\mu) - m_B^2 B_\nu = 0. \tag{38}$$

Taking the divergence of this equation, we find

$$m_B^2 \partial_\mu B_\mu = 0 \tag{39}$$

For the massive case $m_B \neq 0$, B_μ is divergenceless as $\partial_\mu B_\mu = 0$ and Eq.(38) reduces to the Klein-Gordon equation

$$(\Box - m_B^2) B_\mu = 0. \tag{40}$$

The vanishing of $\partial_\mu B_\mu$ means that one of the four degrees of freedom of B_μ is eliminated in a covariant way. In this case, the propagator $\tilde{G}^D_{\mu\nu}(k)$ of the massive vector boson B_μ is derived as

$$\tilde{G}^D_{\mu\nu}(k) \equiv \frac{1}{k^2+m_B^2}\left(\delta_{\mu\nu}+\frac{k_\mu k_\nu}{m_B^2}\right) \tag{41}$$

in the momentum representation [3]. The propagator $G^D_{\mu\nu}(x)$ in the coordinate space is obtained by performing the Fourier transformation as

$$\begin{aligned} G^D_{\mu\nu}(x-y) \equiv \langle B_\mu(x)B_\nu(y)\rangle &= \int \frac{d^4k}{(2\pi)^4} e^{ik\cdot(x-y)}\tilde{G}^D_{\mu\nu}(k) \\ &= \int \frac{d^4k}{(2\pi)^4} e^{ik\cdot(x-y)}\frac{1}{k^2+m_B^2}\left(\delta_{\mu\nu}+\frac{k_\mu k_\nu}{m_B^2}\right). \end{aligned} \tag{42}$$

Here, we consider the scalar-type propagator,

$$\begin{aligned} G^D_{\mu\mu}(x-y) = \langle B_\mu(x)B_\mu(y)\rangle &= \int \frac{d^4k}{(2\pi)^4} e^{ik\cdot(x-y)}\frac{1}{k^2+m_B^2}\left(4+\frac{k^2}{m_B^2}\right) \\ &= \int \frac{d^4k}{(2\pi)^4} e^{ik\cdot(x-y)}\left(\frac{3}{k^2+m_B^2}+\frac{1}{m_B^2}\right) \\ &= 3\int \frac{d^4k}{(2\pi)^4} e^{ik\cdot(x-y)}\frac{1}{k^2+m_B^2}+\frac{1}{m_B^2}\delta^4(x-y)\ , \end{aligned} \tag{43}$$

because $G^D_{\mu\mu}(x-y)$ depends only on the four-dimensional distance $r_{\scriptscriptstyle E} \equiv |x-y|$ and it is convenient to examine $G^D_{\mu\mu}(r_{\scriptscriptstyle E})$ for estimating the mass of the field B_μ. The integration in Eq.(43) is found to be expressed with the modified Bessel function $K_1(z)$,

$$\begin{aligned} I(r_{\scriptscriptstyle E}) \equiv \int \frac{d^4k}{(2\pi)^4} e^{ik\cdot(x-y)}\frac{1}{k^2+m_B^2} &= \frac{1}{(2\pi)^4}\int_0^\infty dk\int_0^\pi d\theta\int_0^\pi d\phi\int_0^{2\pi} d\xi\left(\frac{k^3\sin^2\theta\sin\phi}{k^2+m_B^2}e^{ikr_E\cos\theta}\right) \\ &= \frac{2}{(2\pi)^3}\int_0^\infty dk\frac{k^3\sin^2\theta}{k^2+m_B^2}\left(\int_0^\pi d\theta\sin^2\theta e^{ikr_E\cos\theta}\right) \\ &= \frac{2}{(2\pi)^3}\int_0^\infty dk\frac{k^3}{k^2+m_B^2}\left(\int_{-1}^1 dt\sqrt{1-t^2}e^{ikr_Et}\right) = \frac{1}{(2\pi)^2}\int_0^\infty dk\frac{k^2}{k^2+m_B^2}J_1(kr_{\scriptscriptstyle E}) \\ &= \frac{1}{(2\pi)^2}\frac{m_B}{r_{\scriptscriptstyle E}}K_1(m_Br_{\scriptscriptstyle E}). \end{aligned} \tag{44}$$

Here, we use the integration formula for the Bessel function $J_1(z)$,

$$J_1(z) = \int_{-1}^1 dt\sqrt{1-t^2}e^{izt}, \tag{45}$$

and the formula for the modified Bessel function,

$$zK_1(z) = \int_0^\infty dt\frac{t^2}{t^2+z^2}J_1(t). \tag{46}$$

Thus, the scalar-type propagator $G^D_{\mu\mu}(r_E)$ is written as

$$G^D_{\mu\mu}(r_E) = \frac{3}{4\pi^2}\frac{m_B}{r_E}K_1(m_B r_E) + \frac{1}{m_B^2}\delta^4(x). \tag{47}$$

Using the asymptotic expansion

$$K_1(m_B r_E) \simeq \sqrt{\frac{\pi}{2m_B r_E}}e^{-m_B r_E}\sum_{n=0}^{\infty}\frac{\Gamma(\frac{3}{2}+n)}{n!\Gamma(\frac{3}{2}-n)}\frac{1}{(2m_B r_E)^n}, \tag{48}$$

the scalar-type propagator Eq.(47) reduces to

$$G^D_{\mu\mu}(r_E) \simeq \frac{3\sqrt{m_B}}{2(2\pi)^{\frac{3}{2}}}\frac{e^{-m_B r_E}}{r_E^{\frac{3}{2}}} \tag{49}$$

at the long-range as $r_E > m_B^{-1}$, since the modified Bessel function satisfies the relation $\frac{1}{z}K_1(z) \simeq \sqrt{\frac{\pi}{2}}z^{-3/2}e^{-z}$ for $z > 1$ as shown in Fig.5. In the Eq.(49), the damping factor $e^{-m_B r_E}$ expresses the short-range interaction mediated by the massive field in the coordinate space. Then, the mass m_B of the vector field $B_\mu(x)$ is estimated from the slope in the logarithmic plot of $\frac{r_E^{\frac{3}{2}}}{\sqrt{m_B}}G^D_{\mu\mu}(r_E)$ as the function of r_E,

$$\ln\left\{\frac{r_E^{\frac{3}{2}}}{\sqrt{m_B}}G^D_{\mu\mu}(r_E)\right\} \simeq -m_B r_E + const. \tag{50}$$

B. Numerical Results from Lattice QCD Study

In this subsection, we show the numerical results of the lattice QCD simulation on the propagator and the effective mass of the dual gluon B_μ. For the study of the dual Higgs mechanism in QCD, we numerically calculate the dual gluon propagator $G^D_{\mu\mu}(r_E) \equiv \langle B_\mu(x)B_\mu(x)\rangle_{\mathrm{MA}}$ and try to estimate of the effective mass m_B of the dual gluon field B_μ in the MA gauge using the SU(2) lattice with 24^4 and $\beta = 2.4, 2.45$. All measurements are performed at every 200 sweeps after a thermalization of 10000 sweeps using the heat-bath algorithm. We prepare 60 samples of gauge configurations. These simulations have been performed using NEC SX-4 at Computation Center of Osaka University.

For the effective-mass acquirement of the dual gluon B_μ as the result of infrared monopole condensation, we evaluate the dual gluon propagator obtained from the lattice QCD in the

MA gauge. Since the massive vector-boson propagator is expected to behave as $G^D_{\mu\mu}(r_{\scriptscriptstyle E}) \sim r_{\scriptscriptstyle E}^{-3/2}\exp(-m_B r_{\scriptscriptstyle E})$ at the long distance as shown in Eq.(50), we investigate the logarithm plot of ${r_{\scriptscriptstyle E}}^{3/2} G^D_{\mu\mu}(r_{\scriptscriptstyle E})$ as the function of $r_{\scriptscriptstyle E}$ for the estimation of the dual gluon mass m_B.

We show in Figs.6,7 the lattice QCD data for the dual gluon correlations, $\ln\{r_{\scriptscriptstyle E}^{3/2} G^D_{\mu\mu}(r_{\scriptscriptstyle E})\}$ and $G^D_{\mu\mu}(r_{\scriptscriptstyle E})$, as the function of the 4-dimensional Euclidean distance $r_{\scriptscriptstyle E}$. In Fig.6, the dual gluon correlation $\ln\{r_{\scriptscriptstyle E}^{3/2} G^D_{\mu\mu}(r_{\scriptscriptstyle E})\}$ decreases linearly with $r_{\scriptscriptstyle E}$ in the region of $r_{\scriptscriptstyle E} \gtrsim 0.8$ fm. We try to fit a straight line to the lattice QCD data of $\ln\{r_{\scriptscriptstyle E}^{3/2} G^D_{\mu\mu}(r_{\scriptscriptstyle E})\}$ in this region, and estimate the effective mass m_B of the dual gluon B_μ as $m_B \simeq 0.4$ GeV ($m_B \simeq 0.41$ GeV for $\beta = 2.4$ and $m_B \simeq 0.38$ GeV for $\beta = 2.45$). In Fig.6(b), based on Eq.(50), we compare the dual gluon correlation $\ln\left(r_{\scriptscriptstyle E}^{3/2} G^D_{\mu\mu}(r_{\scriptscriptstyle E})\right)$ with the massive vector-boson correlation with $m_B = 0.4$ GeV in the long distance as $r_{\scriptscriptstyle E} \gtrsim 0.8$ fm. We find good agreement between the lattice QCD data and the massive boson case denoted by the dotted line, and then the dual gluon field B_μ is consider to have the effective mass $m_B \simeq 0.4$ GeV in the infrared region.

In Fig.7, we show the scalar-type dual gluon propagator $G^D_{\mu\mu}(r_{\scriptscriptstyle E}) \equiv \langle B_\mu(x) B_\mu(y)\rangle_{\rm MA}$ in the linear scale. The dotted curve denotes the analytical form in Eq.(47) for the massive vector-boson propagator with $m_B = 0.4$ GeV. In the long-distance region as $r_{\scriptscriptstyle E} \gtrsim$0.8 fm, we find

$$G^D_{\mu\mu}(r_{\scriptscriptstyle E}) \simeq const \cdot \frac{m_B}{r_{\scriptscriptstyle E}} K_1(m_B r_{\scriptscriptstyle E}), \tag{51}$$

and the dual gluon B_μ seems to propagate as the massive vector field with $m_B \simeq 0.4$ GeV. On the other hand, in the short-distance region, $G^D_{\mu\mu}(r_{\scriptscriptstyle E})$ seems to differ from the massive vector propagator. We speculate that such a short-distance deviation on $G^D_{\mu\mu}(r_{\scriptscriptstyle E})$ is brought by the monopole-size effect, because the monopole is considered as a soliton-like object composed of gluons [28].

In this way, we find the effective mass $m_B \simeq 0.4$ GeV of the dual gluon B_μ from the infrared behavior of the dual gluon propagator $G^D_{\mu\nu} \equiv \langle B_\mu(x) B_\nu(y)\rangle_{\rm MA}$ in the MA gauge using the lattice QCD simulation. The effective-mass acquirement of the dual gluon B_μ supports the dual Higgs mechanism by monopole condensation in the QCD vacuum.

VI. SUMMARY AND CONCLUDING REMARKS

In order to clarify the dual superconductor picture for the quark confinement mechanism in the QCD vacuum, we have studied the effective-mass acquirement of the dual gluon field, which is essential for the dual Higgs mechanism. In the maximally abelian (MA) gauge, QCD is reduced into an abelian gauge theory including both the color-electric current and the color-magnetic monopole current.

For the investigation of the dual Higgs mechanism by monopole condensation in QCD, we have introduced the dual gluon field B_μ and have studied its features in the monopole part (the monopole-current system) using the MA gauge in the lattice QCD Monte Carlo simulation. Owing to the absence of the electric current, the monopole part resembles the dual version of QED, and hence this system is naturally described by the dual gluon field B_μ without meeting the difficulty on the Dirac-string singularity. In the dual gauge formalism, the dual Higgs mechanism is characterized by the acquirement of the effective mass m_B of the dual gluon field B_μ. Then, we have investigated the dual gluon mass m_B by examining the inter-monopole potential and the dual gluon propagator, respectively.

As the first attempt to evaluate the dual gluon mass, we have calculated the dual Wilson loop $\langle W_D(R \times T)\rangle_{\rm MA}$, and have studied the inter-monopole potential $V_M(r)$ in the monopole part in the MA gauge by using the lattice QCD simulation. In the lattice QCD, we have found that the dual Wilson loop obeys the perimeter law for large loops. Considering the finite-size effect of the dual Wilson loop, we have numerically derived the inter-monopole potential $V_M(r)$, and have found that $V_M(r)$ is short-ranged and flat in comparison with the linear inter-quark potential. Then, we have compared the inter-monopole potential $V_M(r)$ with the Yukawa potential and have estimated the dual gluon mass as $m_B \simeq 0.5{\rm GeV}$, which is consistent with the phenomenological parameter fitting in the dual Ginzburg-Landau theory [13]. The generation of the dual gluon mass m_B supports the realization of the dual Higgs mechanism and monopole condensation in the QCD vacuum. To explain the short-range deviation between the inter-monopole potential $V_M(r)$ and the Yukawa potential, we have considered the effective size $R_{\rm M}$ of the monopole, which is considered as a soliton-like object composed of gluons. We have found a good agreement of $V_M(r)$ and the Yukawa-type potential $V(r; R_{\rm M})$ with the monopole effective size $R_{\rm M}$ in the whole region of r. The monopole size has been estimated as $R_{\rm M} \simeq 0.2$fm, which would provide the critical scale for the NP-QCD in terms of the dual Higgs theory, because the monopole should be treated as a non-local soliton at the shorter scale than $R_{\rm M}$.

As the second attempt, we have evaluated the effective dual-gluon mass by investigating the dual gluon propagator $G^D_{\mu\mu}(x-y) \equiv \langle B_\mu(x) B_\mu(x) \rangle_{\rm MA}$ in the MA gauge in the lattice QCD. The dual gluon propagator seems to be well fitted by the massive vector-boson propagator at the long distance. From the behavior of the dual gluon propagator in the infrared region, we have estimated the effective dual-gluon mass $m_B \simeq 0.4$ GeV.

Thus, we have shown the effective mass acquirement of the dual gluon field B_μ in the studies of the inter-monopole potential and the dual gluon propagator in the MA gauge using the lattice QCD simulation. This result support the dual Higgs mechanism induced by the monopole condensation, which would be responsible for quark confinement, at the infrared scale of QCD. The values of the dual gluon mass obtained by the two methods seem to coincide within the numerical error. Here, $m_B^{-1} \sim 0.4$ fm corresponds to the "penetration depth" of the dual superconductor and provides the radius of the color-electric flux tube of hadrons [13]. Then, the estimation of the dual gluon mass, $m_B = 0.4 \sim 0.5$ GeV, determines the most relevant quantity of the dual superconducting theory or the key parameter of the dual Ginzburg Landau (DGL) theory [13].

ACKNOWLEDGMENT

We would like to thank Professor Hiroshi Toki for his useful comments and discussions. One of authors (H.S.) is supported in part by Grant for Scientific Research (No.09640359) from the Ministry of Education, Science and Culture, Japan. The lattice QCD simulations have been performed on the super-computer SX4 at Osaka University.

REFERENCES

[1] S. Pokorski, "Gauge Field Theories" (Cambridge University Press, 1985) 1.

[2] For instance, T. P. Cheng and L. F. Li, "Gauge Theory of Elementary Particle Physics" (Clarendon press, Oxford, 1984) 1.

[3] For instance, C. Itzykson and J.-B. Zuber, "Quantum Field Theory" (McGraw-Hill, New York, 1985) 1.

[4] K. Huang, "Quarks, Leptons and Gauge Fields", (World Scientific, Singapore, 1991) 1.

[5] I. J. R. Aitchison and A. J. G. Hey, "Gauge Theories in Particle Physics" (Adam Hilger, Bristol and Philadelphia, 1992) 1.

[6] W. Greiner and A. Schafer, "Quantum Chromodynamics" (Springer,1994) 1.

[7] H. J. Rothe, "Lattice Gauge Theories" (World Scientific, 1992) 1.

[8] Y. Nambu, Phys. Rev. **D 10**, 4262 (1974).

[9] G. 't Hooft, in *High Energy Physics*, edited by A. Zichichi, (Editorice Compositori, Bologna, 1975).

[10] S. Mandelstam, Phys. Rep. **C23**, 245 (1976).

[11] A. A. Abrikosov, "Fundamentals of the Theory of Metals" (Adam Hilger, 1988) 1.

[12] R. W. Haymaker, V. Singh, Y.-C. Peng and J. Wosiek, Phys. Rev. **D 53**, 389 (1996).
V. Singh, D. A. Browne and R. W. Haymaker, Phys. Lett. **B 306**, 115 (1993).

[13] H. Suganuma, S. Sasaki, and H. Toki, Nucl. Phys. **B435**, 207 (1995).
H. Ichie, H. Suganuma and H. Toki, Phys. Rev. **D 52**, 2994 (1995); **D 54**, 3382 (1998).
S. Umisedo, H. Suganuma and H. Toki, Phys. Rev.**D 57**, 1605 (1998).

[14] G. 't Hooft, Nucl. Phys. **B190**, 455 (1981).

[15] Z. F. Ezawa and A. Iwazaki, Phys. Rev. **D 25**, 2681 (1982) ; **D 26**, 631 (1982).

[16] A. S. Kronfeld, G. Schierholz and U.-J. Wiese, Nucl. Phys. **B293**, 461 (1987).

[17] F. Brandstater, U.-J. Wiese and G. Schierholz, Phys. Lett. **B 272**, 319 (1991).

[18] T. Suzuki and I. Yotsuyanagi, Phys. Rev. **D 42**, 4257 (1990).

[19] S. Hioki, S. Kitahara, S. Kiura, Y. Matsubara, O. Miyamura, S. Ohno, and T. Suzuki, Phys. Lett. **B 272**, 326 (1991).

[20] O. Miyamura, Phys. Lett. **B 353**, 91 (1995); Nucl. Phys. **B** (Proc. Suppl.) **42**, 538 (1995).

O. Miyamura and S. Origuchi, “Color Confinement and Hadrons (Confinement ’95)”, edited by H. Toki, Y. Mizuno, H Suganuma, T. Suzuki and O. Miyamura, (World Scientific, 1995) 65.

[21] R. M. Woloshyn, Phys. Rev. **D 51**, 6411 (1995).

[22] T. DeGrand and D. Toussaint, Phys. Rev. **D 22**, 2478 (1980).

[23] J. D. Stack, R. J. Wensley and S. D. Heiman, Phys. Rev. **D 50**, 3399 (1994).

[24] G. S. Bali, V. Bornyakov, M. Muller-Preussker and K. Schilling, Phys. Rev. **D 54** 2863 (1996).

[25] A. Di Giacomo, Nucl. Phys. **B** (Proc. Suppl.) **47**, 136 (1996) and references therein.
M. I. Polikarpov, Nucl. Phys. **B** (Proc. Suppl.) **53**, 134 (1997) and references therein.

[26] H. Suganuma, A Tanaka, S Sasaki and O Miyamura, Nucl. Phys. **B** (Proc. Suppl.) **47**, 302 (1996).

H. Suganuma, M. Fukushima, H. Ichie, and A. Tanaka, Nucl. Phys. **B** (Proc. Suppl.) **65**, 29 (1998).

[27] S. Sasaki and O. Miyamura, Phys. Lett. **B 443**, 331 (1998); hep-lat/9811029, Phys. Rev. **D** in press.

[28] A. Tanaka and H. Suganuma, Proc. of Int. Symp. on “Innovative Computational Methods in Nuclear Many-Body Problems (INNOCOM ’97)”, Osaka, Nov. 1997, (World Scientific) 281.

[29] H. Suganuma, H. Ichie, A. Tanaka and K. Amemiya, Prog. Theor. Phys. Suppl. **131**, 559 (1998).

[30] M. Blagojevic and P. Senjanovic, Nucl. Phys. **B 161**, 112 (1979).

[31] H. Ichie and H. Suganuma, hep-lat/9807025, Nucl. Phys. **B** in press; hep-lat/9808054.

[32] H. Ichie, H. Suganuma and A. Tanaka, Nucl. Phys. **A 629**, 82c (1998).

[33] H. Ichie and H. Suganuma, Proc. of Int. Symp. on “Innovative Computational Methods in Nuclear Many-Body Problems (INNOCOM’ 97)”, Osaka, Nov. 1997, (World Scientific) 278: hep-lat/9802032.

FIGURES

FIG. 1. The dual Wilson loop $\langle W_D(R,T)\rangle_{\rm MA}$ as the function of its perimeter $L \equiv 2(R+T)$ in the monopole part in the MA gauge in the SU(2) lattice QCD with 20^4 lattice and $\beta = 2.3$. The data for the large loops with $R, T > 3$ are shown. The perimeter law seems to hold for $\langle W_D(R,T)\rangle_{\rm MA}$.

FIG. 2. The inter-monopole potential $V_M(r)$ as the function of the distance r between the monopoles in the monopole part in the MA gauge in the SU(2) lattice QCD with 20^4 lattice and $\beta = 2.207, 2.257, 2.3$.

FIG. 3. The logarithmic plot for $rV_M(r)$ as the function of r in the monopole part in the MA gauge in the SU(2) lattice QCD with 20^4 and $\beta = 2.207, 2.257, 2.3$. In the long-distance region, $\ln\{rV_M(r)\}$ seems to decrease linearly with r. For comparison, We plot also the solid line $\ln\{rV_M(r)\} = -m_B r + const$ with $m_B = 0.5$ GeV. The effective mass of the dual gluon B_μ is estimated as $m_B \simeq 0.5$ GeV from the linear slope of $\ln\{rV_M(r)\}$ in the region of $r \gtrsim 0.4$ fm.

FIG. 4. The inter-monopole potential $V_M(r)$ as the function of the distance $r \equiv |\mathbf{x}-\mathbf{y}|$ between the monopoles in the SU(2) lattice QCD with 20^4 and $\beta = 2.207, 2.257, 2.3$. The dotted and the solid curves denote the simple Yukawa potential $V_{\rm Y}(r)$ and the Yukawa-type potential $V(r;R_{\rm M})$ with the monopole size effect, respectively. The Yukawa-type potential $V(r;R_{\rm M})$ seems to fit the inter-monopole potential $V_M(r)$ with the effective monopole size $R_{\rm M} \simeq 0.2$fm in the whole region of r.

FIG. 5. (a) The function $G(z) \equiv \frac{1}{z}K_1(z)$ (solid curve) appearing in the massive boson propagator and its asymptotic form $\sqrt{\frac{\pi}{2z^3}}e^{-z}$ (dotted curve) as the function of z. (b) The logarithmic plots for $z^{3/2}G(z) = \sqrt{z}K_1(z)$ (solid curve) and $\sqrt{\frac{\pi}{2}}e^{-z}$ (dotted line) as the function of z. For $z > 1$, the function $G(z)$ is apporoximated by its asymptotic form as $G(z) \simeq \sqrt{\frac{\pi}{2z^3}}e^{-z}$.

FIG. 6. (a) The logarithmic plot of ${r_{_E}}^{3/2}G^D_{\mu\mu}(r_{_E})$ as the function of $r_{_E}$ in the monopole part in the MA gauge in the SU(2) lattice QCD with 24^4 and $\beta = 2.4, 2.45$. The correlation $\ln\left(r_{_E}^{3/2}G^D_{\mu\mu}(r_{_E})\right)$ decreases linearly with $r_{_E}$ in the long-distance region. (b) The comparison with the analytical form in Eq.(47) for the massive vector-boson propagator with the mass $m_B = 0.4$ GeV. The massive-boson correlation denoted by the dotted line almost reproduces the lattice QCD data for the dual gluon correlation $\ln\left(r_{_E}^{3/2}G^D_{\mu\mu}(r_{_E})\right)$ at the long distance as $r \gtrsim 0.8$ fm. The effective mass of the dual gluon is estimated as $m_B \simeq 0.4$ GeV from the linear slope of $\ln\left(r_{_E}^{3/2}G^D_{\mu\mu}(r_{_E})\right)$ in the infrared region.

FIG. 7. The scalar-type dual gluon propagator $G^D_{\mu\mu}(r_{_E})$ as the function of the 4-dimensional Euclidean distance $r_{_E}$ in the monopole part in the MA gauge in the SU(2) lattice QCD with 24^4 and $\beta = 2.4, 2.45$. The dotted curve denotes the propagator of the massive vector boson with the mass $m_B = 0.4$ GeV. The dual gluon B_μ seems to propagate as the massive vector field at the long distance as $r_{_E} \gtrsim 0.8$ fm.

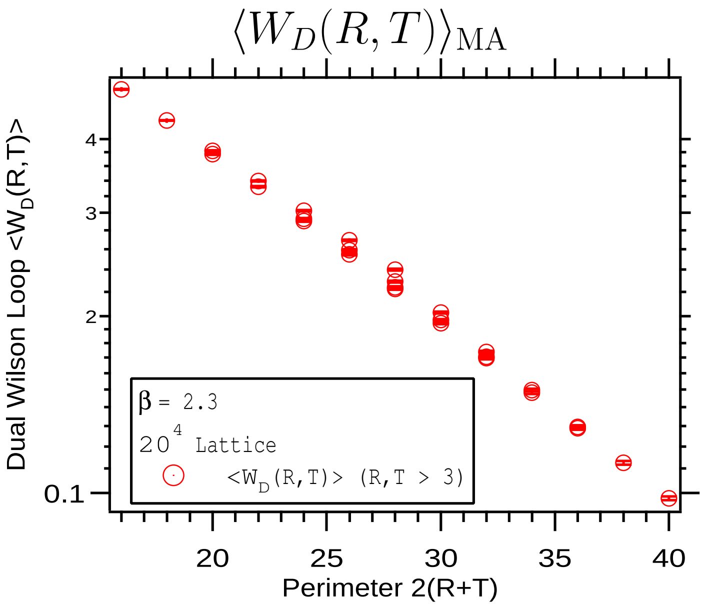
$\langle W_D(R,T)\rangle_{\rm MA}$
Dual Wilson Loop <W_D(R,T)>
4
3
2
0.1
20
25
30
35
40
Perimeter 2(R+T)
β = 2.3
20^4 Lattice
<W_D(R,T)> (R,T > 3)

Figure 1

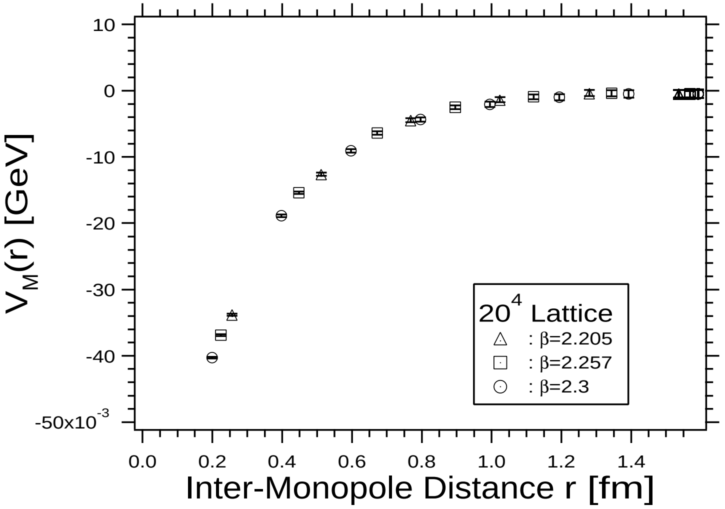

Inter-Monopole Potential $V_M(r)$

Figure 2

$\ln\{rV_M(r)\}$

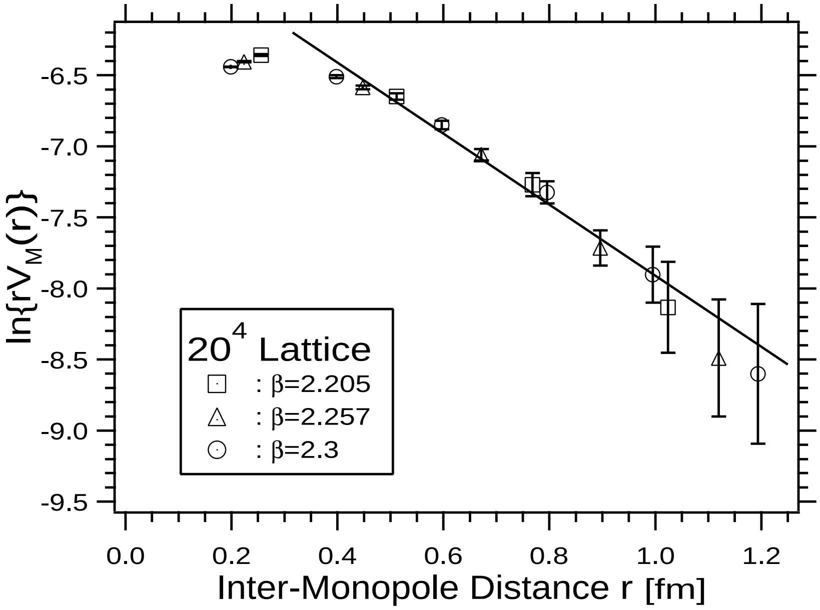

Figure 3

Inter-Monopole Potential $V_M(r)$

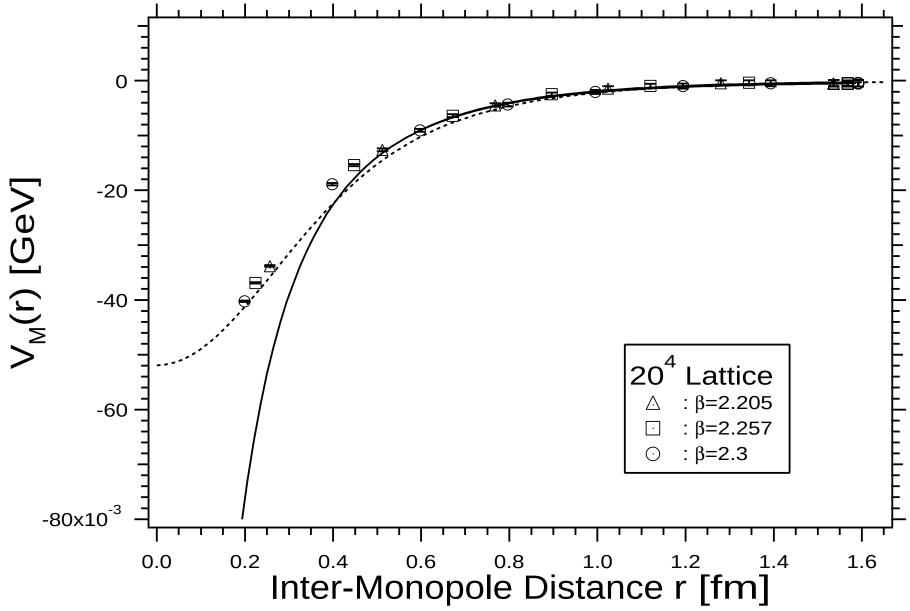

Figure 4

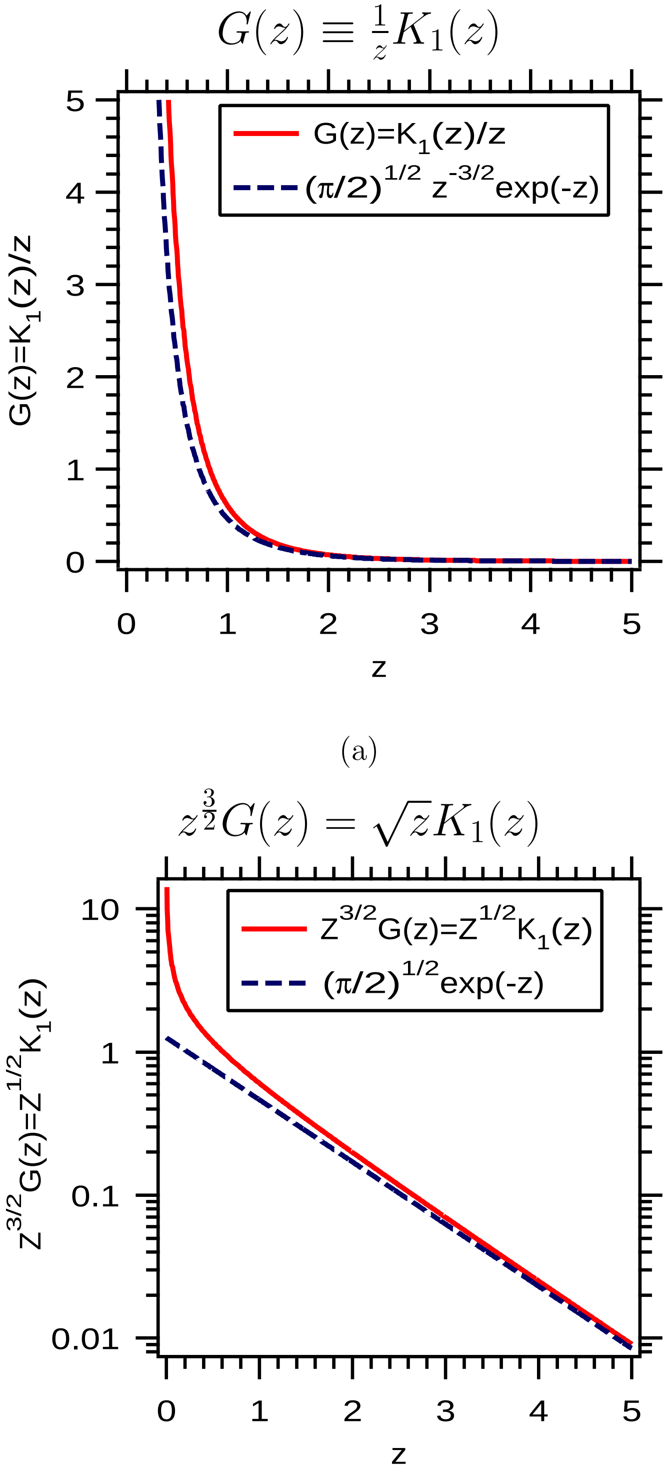
$G(z) \equiv \frac{1}{z}K_1(z)$
G(z)=K1(z)/z
(π/2)1/2 z-3/2exp(-z)
G(z)=K1(z)/z
5
4
3
2
1
0
0
1
2
3
4
5
z
$z^{\frac{3}{2}}G(z) = \sqrt{z}K_1(z)$
Z3/2G(z)=Z1/2K1(z)
(π/2)1/2exp(-z)
Z3/2G(z)=Z1/2K1(z)
10
1
0.1
0.01
0
1
2
3
4
5
z

(a)

(b)

Figure 5

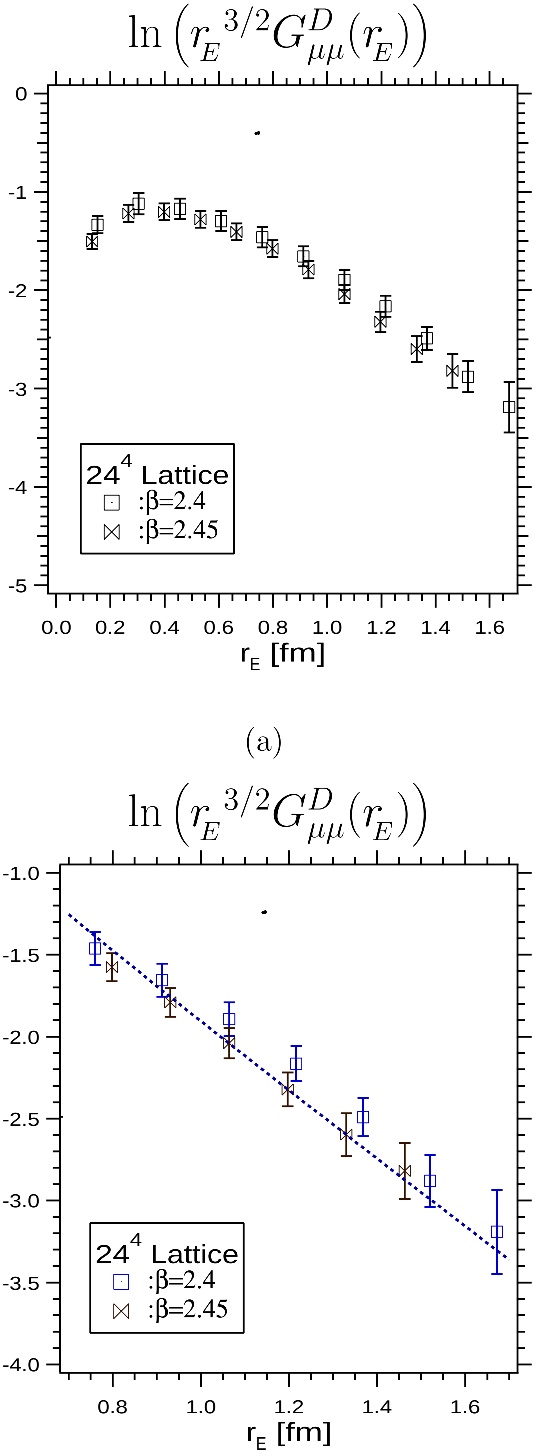

$\ln\left(r_E^{\,3/2} G^D_{\mu\mu}(r_E)\right)$

(a)

$\ln\left(r_E^{\,3/2} G^D_{\mu\mu}(r_E)\right)$

(b)

Figure 6

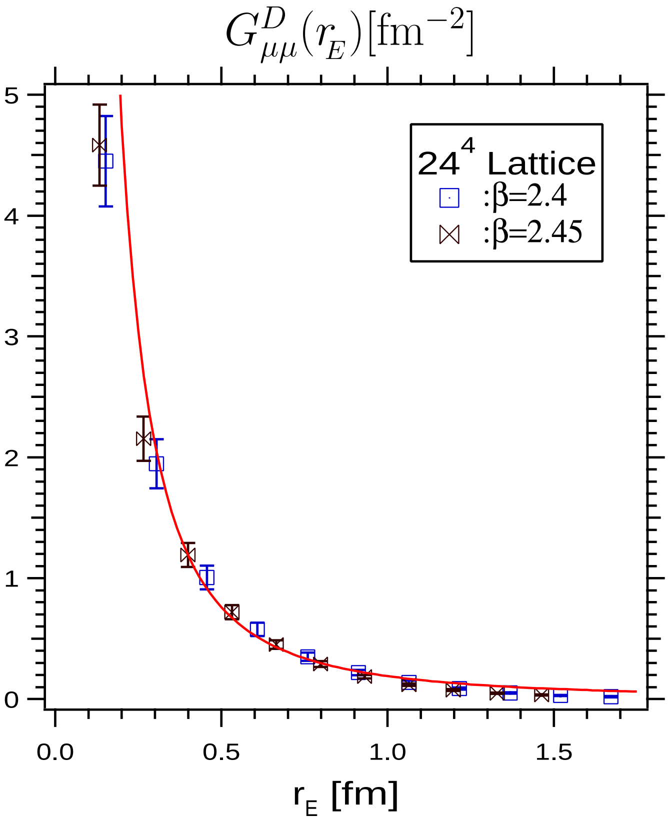
$G^D_{\mu\mu}(r_E)[\mathrm{fm}^{-2}]$
5
4
3
2
1
0
0.0
0.5
1.0
1.5
r_E [fm]
24^4 Lattice
:β=2.4
:β=2.45

Figure 7